Transport of large Particles and Macromolecules in Flow Through Inorganic Membrane

A. O. Imdakm and T. Matsuura

Department of Chemical Engineering, University of Ottawa, 161 Louis Pasteur St., Ottawa, Ont., Canada KIN 6N

Abstract

The influence of transport of large particles and macromolecules on membrane separation efficiency and permeation rate limitation has been observed in many separation processes of microscopic scale. In this paper a Monte Carlo simulation model is developed to study this phenomenon. The membrane pore space is described by a three-dimensional network model of inter-connected cylinders pores. The effective radii of these pores are distributed according to experimentally reported pore size distribution. The paths of the injected particles throughout the pore space are determined by transition probability function proportional to the pore flux. Pores are considered completely blocked when particles of effective radii comparable with the pore size pass through them. Thus, the membrane capability of transport can ultimately vanish and, therefore, this process is a percolation process and it is characterized by a percolation threshold below which the membrane losses its macroscopic connectivity. When the model applied to this problem, the predictions are in excellent agreement with the available experimental data.

***Keywords*:** Ultrafiltration; Network model; Suspensions; Macromolecules; Permeability Reduction; Size Exclusion; SE.

1 Introduction

In recent years, there is a wide spread of commercial development in separation processes utilizing membranes in large area of industrial interest. In many of such transport operations in chemical and biochemical industries involve separation of large particles and macromolecules in restricted environment. For example, reverse osmosis (RO), micro-filtration (MF), ultra-filtration (UF), and deep-bed filtration (DBF). The efficiency of such process, which is the point of interest of this study, depends crucially on the availability of an open membrane pore space through which mass transport takes place. Thus, if such transporting paths (pore spaces) are reduced during the separation process, the permeation rate, which is considered as one of the measures of membrane performance, is reduced. As a result, the whole separation operation is also reduced to a certain degree depending on the degree of pore space reduction.

In many separation processes as in MF/UF, the most important issue is the transport of large particles and macromolecules whose effective radii are comparable to the pore size of the membrane. These transporting particles and macromolecules can be the component of the feed fluid or sometimes they can also arise due to the release of material deposited on the membrane pore walls or due to chemical reaction between the flowing fluid and membrane pore wall, which may take place because of the change in transporting fluid ionic environments. When emulsions droplets are present in flow of stable emulsions such as those in oily wastewater, paints, starch, and skim milk, significant number of membrane pores can also be blocked by emulsions droplets, the sizes of which are comparable to membrane pore sizes. This type of membrane pore plugging by solid particles or emulsions droplets of effective sizes comparable to the size of the membrane pores is known as pore plugging by **size-exclusion (SE)**. This mechanism of membrane pore space reduction is found to be the most dominant mechanism of flux rate reduction in many cases [1,3,4,5]. The capture of particles or emulsions droplets by pore wall because of electrical interaction between them is another mechanism of pore space reduction, but pore plugging by size exclusion mechanism still plays the most fundamental role in pore space reduction. Interesting reader may referred to the excellent reviews of Belfort et al. [2] and M. Sahimi et al. [5] for the theoretical models describing the transport processes in flow through porous media, their validity and limitation. These models in general ignore the detail descriptions of the membrane pore space (morphology), and the phyisco-chemical interaction between the transporting particles and membrane pore wall.

In this study an attempt is made to predict the performance of ultrafiltration membranes with the assumption that the pore space reduction is only due to size exclusion, SE, mechanism. SE is believed to be one of the primary reasons for the membrane pore space reduction and a thorough study based on SE will give some insight into the fouling phenomena by membrane pore space reduction. The calculation carried out in this study is also based on the parameters describing the pore size distribution obtained by Wang et al. [6]. Agreement of calculation and experimental data is further examined.

2 Model Formulations

2.1 Membrane pore space

The membrane pore space is described by simple-cubic (**L x L x L, L=12**) network model in which the bonds of the network represent the pore-throat. Each pore is assumed to be a cylindrical tube of constant length *l* and an effective diameter D_{pore}. The initial effective diameter of these pores are distributed according to a lognormal probability density function with geometric mean pore size μ_{pore} and standard deviation σ_{pore} as reported by Wang et al. [6]. The geometrical mean pore size and standard deviation are listed in **Table-1.** The sizes of the sites, which represent the pore bodies, are

$$\frac{df(D_{pore})}{dD_{pore}} = \frac{1}{D_{pore}(ln\sigma_{pore})\sqrt{2\pi}} \exp\left[\frac{(lnD_{pore}-ln\mu_{pore})^2}{2(ln\sigma_{pore})^2}\right] \quad (1)$$

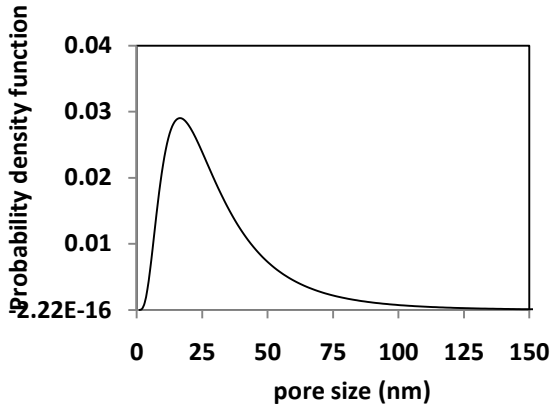

Figure 1: Probability density function for membranes 0.5 A..

assumed to be large enough in order to be able to contain the transporting particles. The pore length was estimated based on the mean pore length determined microscopically, Wang et al. [6]. Creping flow within each pore is assumed, as such, the volumetric flow rate q_i of pore *i* is defined as $q_i = g_i \Delta p_i$ where Δp_i is pressure drop across the pore and g_i is the hydraulic conductance of the pore, which is proportional to R_{pore}^4. The boundary conditions are constant pressure drop as given experimentally, Wang et al. [6], imposed in the z-direction, and periodic boundary condition in the X and Y direction.

Therefore, steady state pressure distribution in the entire network can be computed. From the pressure distribution, one can calculate network permeability, average flow velocity, flow rate in each pore, the time needed for the suspended particles to pass through the pore, and cross-flux (permeate) using experimentally reported surface porosity shown in Table-1**.**

Thickness (μm) "Calcinations effect" Before	After	μ_{pore} (nm)	σ_{pore}	Surface Porosity (%)
97	85	25.7	1 .95	3.15

Table 1: Properties of Sepiolite Membrane (0.5 A) as given by Wang et al. [6].

2.2 Particles sizes

The macromolecules solutes, which are injected into the network, are polyethylene glycol PEG, (A), and polyethylene oxide PEO, (B), (C), (D), and (E) . They are assumed to be spheres with radii estimated from the **Einstein-Stock** equation depending on their molecular weight, Mw, (see table-2).

Molecular weight	Macromolecules radius $r_p x10^9$ (m)
35,000 (A)	5.6825
100,000 (B)	8.9888
200,000 ©	13.5022
300,000 (D)	17.1305
400,000 (E)	20.282

Table 2**:** Radius of injected molecules, r_p. based on Einstein-Stocks equation.

Thus, for PEG

$$r_p = 16.73x10^{-12}M_w^{0..557}, \quad (2)$$

and for PEO

$$\cdot r_p = 10.44x10^{12} M_w^{0.587} \quad (3)$$

2.3 Particles Movement

Suppose $V_{pore}\tau$ of fluid comes into the membrane within time interval Δt, where V_{pore} is the total volume of the network bonds at initial condition (i.e., at t=0), and τ is the number of pore volumes being injected into the network. The time interval Δt can be given as $V_{pore}\tau/Q$, where Q is the volumetric flow rate of the fluid coming into the network, and Δt can be defined as the time needed to inject such amount of constant volume of fluid ($V_{pore}\tau$). Q decreases with time because of pore plugging by SE that increases with time t. Therefore, Δt will increase with an increase in time until the system reaches steady state condition (i.e., no more pore plugging). The number of particles, M, being injected into the network within the time interval Δt is assumed to be constant (constant solute concentration) as reported experimentally (Wang et al. [6]), and it can be calculated given solute concentration (ppm), $V_{pore}\tau$, r_p, and particles density, ρ_p. Once the particle is injected at the network entrance (Z=o), it moves in the Z-direction to the next node, this because of the constant pressure drop imposed in the Z-direction, or it may cause pore plugging by SE (if $r_p \geq R_{pore}$) (rejection).When the particle arrived at anode, it moves to the one of the unplugged pores attached to this node with probability proportional to the fraction of flow rate departing from the node through this pore. Once the pore is chosen, the effective radius, r_p, of the particle is compared with the radius of the selected pore, R_{pore}. If $r_p \geq R_{pore}$, the pore entrance considered totally blocked by the solid particle (setting its radius to zero), this is equivalent to removing that bond from the network. If $r_p < R_{pore}$, the particle is allowed to pass through the pore to the next node. It is clear that this process is a percolation process. Once a set of plugged pores are identified, a new flow filed is computed, taking into consideration the presence of all the solid particles and their effect on the flow field.

3 Results and Discussion

In this study, an extensive Monte Carlo simulation of this process described above is carried out; it is obvious that the sharp permeability reduction observed experimentally (Wang et al. [6]) is due to the significant pore plugging mainly by SE.

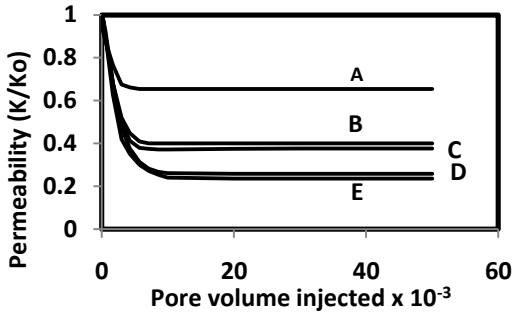

Figure 2: Normalized permeability vs. pore volume injected.

This is may due the fact that the injected particles are of size r_p that is comparable to the mean pore size, μ_{pore}, and as such, a large fraction of pores are plugged by SE and in particular at network entrance. Figure 2 shows clearly the permeability reduction observed in the early stage of the ultra- filtration. It decreases quickly due to SE in the first stage of filtration and reaches steady state after some time.

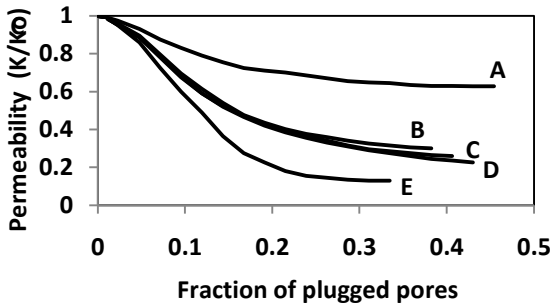

Figure 3: Normalized permeability of Figure 2 vs. fraction of plugged pores.

The results are carried out for operating pressure of 55 psig. The permeability changes with the fraction of pores plugged is given in Figures 3. This figure show that permeability decrease quickly until about 20% of the pores are blocked particularly in close vicinity to the network entrance and then level off slowly due to small fraction of pore plugging deep down into the network. Figure 4 show the flux rate of pure water and the flux decline due to the injection of solutes of different molecular weights and under different operating pressures. Experimental results are also shown on the same figure. The agreement between the experimental and calculated data is excellent in a pressure range 35-115 psig.

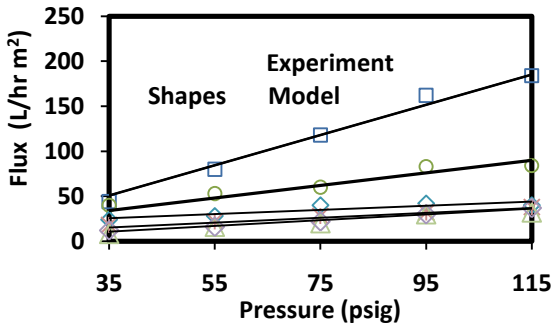

Figure 4: Comparison of predicted flux rates vs. pressure with the experimental data. □ pure water, ○ A, ◊ B&C, x D, and Δ E , Wang et al. [6].

The number of particles, M, injected into the pore network during the time interval Δt, not all of them will pass through the network. Some of them get rejected at the network entrance, other will cause pore plugging within the network (and may cause also particles trapping within the plugged pores, and the rest will eventually pass through the network. As the system approach steady state, the particles which may cause pore plugging decrease. When the steady reached, all the particles injected will take relatively a long path and time period far larger than the given time interval Δt before they can pass through the network. If the number of particles passing through the network during the time interval Δt becomes M_{out}, thus after steady state is reached, $1 - M_{out}/M$ is the separation of particles by the network, The separation plotted versus the molecular weight of the macromolecules solutes in Figure 5 does not show any applied pressure dependence. The results confirmed clearly by reported experimental data.

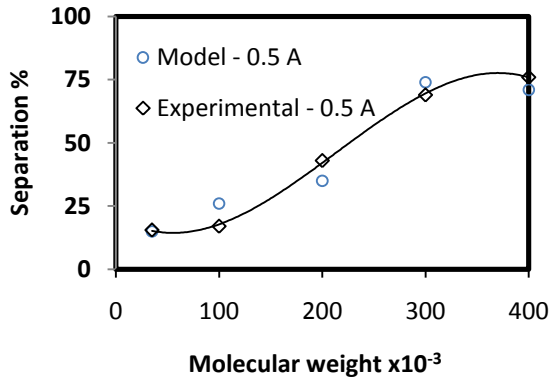

Figure 5: Comparison of steady state separation with experimental data , Wang et al. [6].

4 Conclusions

From the results presented above, we can draw the following conclusion:

- The Monte Carlo simulation model based the transport through three-dimensional network model of interconnected pores can describe the experimental ultra-filtration data both qualitatively and quantitatively *without resorting to any adjustable parameters*.
- According to the network model prediction, the membrane pore is blocked mainly by size exclusion, SE, mechanism, which results in the *sever reduction* of the permeability (flux rate) during the first a few seconds.

5 References

[1] Baghdikian S, Y,, Sharma M. M., ana Handy L. L., "Flow of clay suspensions through porous media." SPE 16257, Denver, CO., (1987).

[2] Belfort, G., R. Davis. And A. L. Zydeny, "The behavior of suspensions and macromolecular solutions in crossflow microfiltration," J. Membr. Sci., 96 1(1994).

[3] Imdakm, A. O., and M. Sahimi, "Transport of large particles in flow through porous media." Phys. Rev., A 36, 3099 (1987).

[4] Imdakm, A. O., and M. SAhimi, "computer simulation of particle transport processes in flow through porous media," Chem. Eng. Sci. 46, 1977 (1991).

[5] Sahimi M., and A. O. Imdakm, "The effect of morphological disorder on hydrodynamic dispersion in flow through porous media," J. Phys., A21, 3833 (1988).

[6] Wang Q. K., T. Matsuura, C. y. Feng, M. R. Weir, C. Detellier, E. Rutadinka, and R. L. Van Mao, "The sepiolite membrane for ultrafilteration,"J. Membr. Sci. 184, 153 (2001).